'Effect of Indium Doping on Surface Optoelectrical Properties of Cu2ZnSnS4 Photoabsorber and Interfacial/Photovoltaic Performance of Cadmium Free In2S3/Cu2ZnSnS4 Heterojunction Thin Film Solar Cell

Submission date: 24-Nov-2020 02:46PM (UTC+0700)
Submission ID: 1455907011
File name: C-8_oke.pdf (2.97M)
Word count: 7293
Character count: 37958

by Gunawan Gunawan

CHEMISTRY OF MATERIALS

Article

pubs.acs.org/cm

Effect of Indium Doping on Surface Optoelectrical Properties of Cu_2ZnSnS_4 Photoabsorber and Interfacial/Photovoltaic Performance of Cadmium Free In_2S_3/Cu_2ZnSnS_4 Heterojunction Thin Film Solar Cell

Feng Jiang,[†] Chigusa Ozaki,[†] Gunawan,[†] Takashi Harada,[†] Zeguo Tang,[‡] Takashi Minemoto,[‡] Yoshitaro Nose,[§] and Shigeru Ikeda*[,†,∥]

[†]Research Center for Solar Energy Chemistry, Osaka University, 1-3 Machikaneyama, Toyonaka, Osaka 560-8531, Japan

[‡]Department of Electrical and Electronic Engineering, Faculty of Science and Engineering, Ritsumeikan University, 1-1-1 Nojihigashi, Kusatsu, 525-8577, Japan

[§]Department of Materials Science and Engineering, Kyoto University, Yoshida-Honmachi, Sakyo-ku, Kyoto 606-8501, Japan

Supporting Information

ABSTRACT: Maximum conversion efficiency of 6.9% was obtained over an electrodeposited Cu_2ZnSnS_4-based thin film solar cell with a Cd-free In_2S_3 buffer layer by applying a rapid post-heat treatment to the In_2S_3/Cu_2ZnSnS_4 stacked layer. It was found that post-heating of the In_2S_3/Cu_2ZnSnS_4 stack promoted an increment of the acceptor density of the Cu_2ZnSnS_4 layer close to the In_2S_3–Cu_2ZnSnS_4 heterointerface of the In_2S_3/Cu_2ZnSnS_4 stack. Moreover, the diffusion of In also resulted in a red-shift of the band gap energy of Cu_2ZnSnS_4 from 1.47 to 1.40 eV. Due to extension of external quantum efficiency response of the solar cell to the long wavelength region, the solar cell based on the post-heated In_2S_3/Cu_2ZnSnS_4 stack reached appreciably large short circuit current density of more than 20 mA cm^{-2}. The energy difference between the conduction band minimum of In_2S_3 and that of Cu_2ZnSnS_4 at the In_2S_3/Cu_2ZnSnS_4 heterointerface was determined to be a slightly positive value of 0.11 eV, indicating formation of a "notch-type" conduction band offset for efficient suppression of the interface recombination.

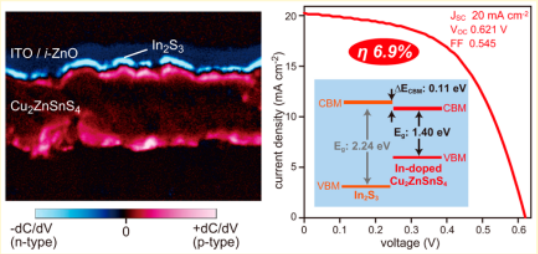

1. INTRODUCTION

Kesterite Cu_2ZnSnS_4 has attracted much interest as a promising light-absorbing material for next-generation photovoltaic devices because of its optimal photoelectric properties such as a high photoabsorption coefficient and ideal band gap energy for efficient sunlight absorption with theoretical light-to-electrical power conversion efficiency (η) of above 30%.[1−5] Although maximum η's of currently available devices are only 9%,[6−8] a Cu_2ZnSnS_4-based solar cell would be the leading candidate for an alternative to the current $Cu(In,Ga)(Se,S)_2$-based solar cell because constituent elements of the absorber are not rare and are less toxic.[9−28] However, one critical problem for the use of a Cu_2ZnSnS_4-based solar cell is that a toxic CdS buffer layer has been used in almost all of the reported solar cells with relatively high efficiencies. Besides, the CdS buffer is not likely to be the best candidate to fabricate a highly efficient Cu_2ZnSnS_4-based solar cell from the viewpoints of conduction band offset (CBO),[29−32] leading to appreciable interface recombination of photoexcited carriers. Therefore, the CdS buffer should be replaced with other environmentally favorable compounds having adequate structural and electronic properties.

As a good substituent of the CdS buffer layer to prepare an efficient Cu_2ZnSnS_4-based solar cell, the compound should have sufficient transparency of sunlight radiation in the absorption range of Cu_2ZnSnS_4. An electrical property suitable for efficient transfer of photoexcited electrons from the Cu_2ZnSnS_4 absorber is also required. Zinc sulfide (ZnS), indium sulfide (In_2S_3), and their partially oxidized forms are promising candidates because ZnS has an appreciably wide band gap (3.6 eV) and In_2S_3 has a low photoabsorption coefficient due to its indirect semiconductive characteristic despite its relatively narrow band gap (2.1 eV).[33−35] In fact, these compounds have been proved to work as efficient buffer layers for a $Cu(In,Ga)(Se,S)_2$-based solar cell. For applications to a Cu_2ZnSnS_4-based solar cell, record efficiencies of 5.8% and 6.3% were achieved by Hiroi et al. using ZnS-based and In_2S_3-based buffer layers, respectively.[35] In both cases, appropriate surface treatments of Cu_2ZnSnS_4 were shown to be effective for obtaining better solar cell performances, though there has been

Received: December 24, 2015
Revised: April 19, 2016

   DOI: 10.1021/acs.chemmater.5b04984
Chem. Mater. XXXX, XXX, XXX−XXX

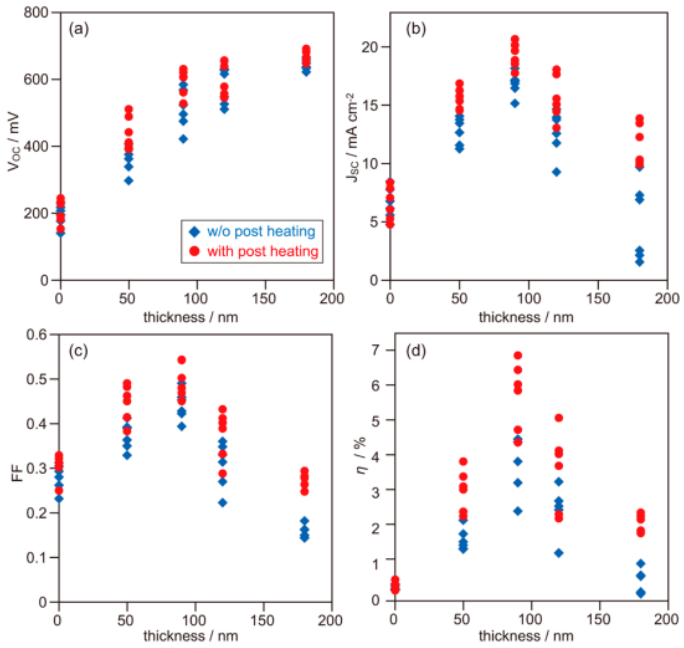

Figure 1. (a) V_{OC}, (b) J_{SC}, (c) FF, and (d) η of In_2S_3/Cu_2ZnSnS_4-based solar cells with different thicknesses of In_2S_3 layers without and with applying post-heat treatment at 300 °C in air for 1.5 min.

no structural/electrostructural information to explain effects of such treatments. Since a relatively favorable CBO was expected based on spectroscopic analyses of the In_2S_3/Cu_2ZnSnS_4 heterointerface,[32] solar cell properties based on the In_2S_3/Cu_2ZnSnS_4 heterointerface were discussed by other groups. However, the reported efficiencies have not achieved η of larger than 2%,[32,36] and thus further improvements of conversion efficiency by optimizing deposition conditions and/or adding appropriate treatments are needed. In this study, therefore, we focused on the use of an In_2S_3-based buffer layer, which was deposited by a chemical bath deposition (CBD) technique using an acidic bath. Specifically, effects of applying a post-heat treatment to the In_2S_3/Cu_2ZnSnS_4 stack on solar cell performances are discussed in relation to structural, electric, optical, and electroenergetic properties.

2. EXPERIMENTAL SECTION

Preparation of a Cu_2ZnSnS_4 Thin Film. Cu_2ZnSnS_4 films used in this study were obtained by sulfurization of preannealed electrodeposited Cu/Sn/Zn stacks on a Mo-coated glass substrate. The detailed procedure has been reported previously.[22−24] Briefly, on a Mo-coated soda lime glass substrate (Mo/glass), Sn(II) methanesulfonate and Zn(II) sulfate, respectively, were deposited by a potentiostatic mode using an electroplating bath containing Cu(II) sulfate. After heating thus-obtained Cu/Sn/Zn precursor stacks at 310 °C for 200 min in an evacuated borosilicate glass ampule, these precursors were sealed again in an evacuated borosilicate glass ampule containing sulfur powder; the ampule was then put in a 590 °C heated furnace for 10 min to facilitate sulfurization. As confirmed by inductively coupled plasma (ICP) analysis using a PerkinElmer OPTIMA 3000-XL ICP emission spectrometer, Cu/(Sn + Zn) and Zn/Sn ratios of used Cu_2ZnSnS_4 thin films were 0.85 and 1.15, respectively.

Device Fabrication. The thus-obtained Cu_2ZnSnS_4 film with the thickness of about 1.2 μm deposited on Mo/glass was treated with 1 mol dm^{-3} aqueous potassium cyanide (KCN) solution for 1 min. Then the sample was immersed in an a solution composed of 25 mol dm^{-3} indium sulfate, 0.1 mol dm^{-3} thioacetamid, and 0.1 mol dm^{-3} acetic acid at 65 °C to form an In_2S_3-covered Cu_2ZnSnS_4 sample. Thickness of the In_2S_3 layer was controlled from 50 to 180 nm by changing the deposition duration from the 8 to 30 min, e.g., a 90 nm-thick In_2S_3-covered Cu_2ZnSnS_4 was obtained by deposition of In_2S_3 for 15 min (Figure S1). Some of the In_2S_3-covered Cu_2ZnSnS_4 samples were subjected to being put onto a hot plate preheated at 300 °C for 1.5 min in open air. An ITO/ZnO bilayer was deposited on top of the In_2S_3 layer by radio frequency (RF) magnetron sputtering. Finally, Al back contact was deposited by evaporation to form a device with a structure Al/ITO/ZnO/In_2S_3/Cu_2ZnSnS_4/Mo/glass.

Characterizations. Current density−voltage (J−V) and external quantum efficiency (EQE) characteristics of solar cells were determined in air with a Bunkoh-Keiki CEP-015 photovoltaic measurement system under a simulated amplitude modulation of AM 1.5G irradiation (100 mW cm^{-2}). XP spectroscopy was performed by using a Shimadzu AXIS ULTRA X-ray photoelectron spectrometer in monochromated Al Kα radiation. The Ar^+ ion etching was performed at beam energy of 3.7 keV. Depth profiles of Cu, In, Mo, S, Sn, and Zn elements in typical 90 nm-thick In_2S_3-covered Cu_2ZnSnS_4 films were analyzed by using a ULVAC-PHI SAM-670 Auger Electron Microscope. For this measurement, the Ar^+ ion etching was also performed at beam energy of 3.0 keV. Depth profiles of In and Cu in these films were also analyzed by using a HORIBA GD-Profiler2 rf-GDOES apparatus. Scanning capacitance microscopy (SCM) measurements were performed by using a Digital Instruments Dimension 3100 scanning probe microscope equipped with an Nanoscope IVa controller and an SCM application module. Capacitance−voltage (C−V) characteristics of typical solar cells based on 90 nm-thick In_2S_3-covered Cu_2ZnSnS_4 films were measured by using a HP-HEWLETT PACKED 4284A apparatus. Photoluminescence (PL) spectra of these films were obtained by using a Hamamatsu C12132 Compact NIR Fluorescence Lifetime Spectroscopy System with laser power and wavelengths of 2.08 mW and 532 nm, respectively.

DOI: 10.1021/acs.chemmater.5b04984
Chem. Mater. XXXX, XXX, XXX−XXX

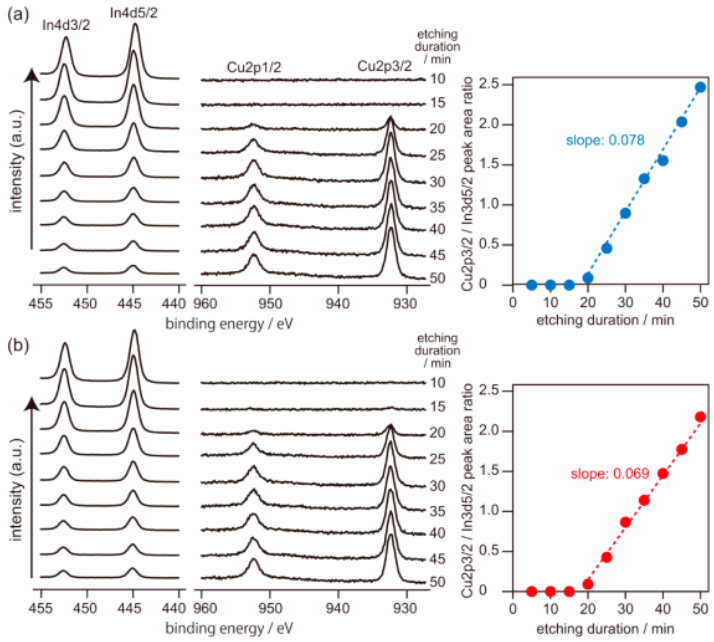

Figure 2. Left: Cu 2p and In 3d XP spectra of (a) In_2S_3−Cu_2ZnSnS_4_w/o and (b) In_2S_3−Cu_2ZnSnS_4_PH films after Ar^+ etching with various durations. Right: plots of peak area ratios of Cu 2p3/2 to In 3d5/2 as a function of Ar^+ etching duration.

3. RESULTS AND DISCUSSION

3.1. Effects of Post-Heating on Solar Cell Properties. The Cu_2ZnSnS_4 absorber used in this study was obtained by an electrochemical technique reported previously: the Cu_2ZnSnS_4-based solar cell gave the best η of more than 8% upon combination of the conventional CdS buffer layer.[24] In this study, In_2S_3 buffer layers with different thicknesses were deposited by CBD, and solar cells were fabricated by subsequent depositions of ZnO and indium tin oxide (ITO) layers and an Al top contact. Averages of open circuit voltage (V_{OC}), short circuit current density (J_{SC}), fill factor (FF), and η of several Cu_2ZnSnS_4-based solar cells fabricated by using the CBD-deposited In_2S_3 buffer layers with different thicknesses are plotted as filled markers in Figure 1. Compared to the cell fabricated without deposition of In_2S_3 (i.e., In_2S_3 thickness of 0 nm), deposition of an In_2S_3 buffer significantly improved all of the parameters, though a relatively thick In_2S_3 buffer layer (180 nm) greatly reduced J_{SC} and FF probably due to its high level of resistance. The best cell with V_{OC}, J_{SC}, FF, and η of 585 mV, 17 mA cm^{-2}, 0.450, and 4.5% was obtained by using a 90 nm-thick In_2S_3 buffer layer. Since a cell using a CdS buffer layer was reported to have relatively high values of V_{OC} (705 mV), J_{SC} (18 mA cm^{-2}), and FF (0.632),[24] it should be possible to improve such device parameters by modifying the In_2S_3 layer and/or the In_2S_3−Cu_2ZnSnS_4 heterointerface. For this purpose, we applied an open-air heat treatment at 300 °C in air for 1.5 min just after deposition of In_2S_3 during fabrication of the solar cell. Average solar cell parameters of resulting devices with different thicknesses of the In_2S_3 layer are shown as red markers in Figure 1. Regardless of the In_2S_3 thickness, all of the parameters were improved by applying the post-heating. As expected from the above results for the cell without application of the post-heating, the best cell with V_{OC}, J_{SC}, FF, and η of 621 mV, 20 mA/cm^2, 0.545, and 6.9%, respectively, was obtained by using a 90 nm-thick In_2S_3 buffer layer. To the best of our knowledge, the achieved η is the highest for Cd-free Cu_2ZnSnS_4-based thin-film solar cells reported so far. When focusing on solar cell parameters of the cell without In_2S_3, there was no significant improvement in any of the parameters by post-heating, suggesting that the post-heating modulates structural and electric properties of the In_2S_3 buffer, the In_2S_3−Cu_2ZnSnS_4 heterointerface (i.e., the depletion region of Cu_2ZnSnS_4), and/or bulk properties of Cu_2ZnSnS_4.

3.2. Changes in Properties Induced by Post-Heating. Figure 2 shows Cu 2p and In 3d XP spectra of the typical 90 nm-thick-In_2S_3-deposited Cu_2ZnSnS_4 films without and with post-heating (labeled In_2S_3(90)/Cu_2ZnSnS_4_w/o and In_2S_3(90)/Cu_2ZnSnS_4 _PH, respectively) after etching with argon ion (Ar^+) for various durations. In both samples, intense In 3d peaks were solely observed for both samples after Ar^+ etching shorter than 15 min; they gradually decreased with increase in the etching duration accompanied by monotonic increases in Cu 2p peaks. Similar results were also obtained for Sn 3d and Zn 2p peaks, as shown in Figure S2a. In addition, there was almost no oxygen component observed in the Ar^+-etched samples: both In_2S_3(90)/Cu_2ZnSnS_4_w/o and In_2S_3(90)/Cu_2ZnSnS_4 _PH showed appreciable oxygen mainly at their external surfaces (Figure S2b). Moreover, all of the metallic elements in both Ar^+-etched samples appeared at fixed chemical shifts. These results indicate that there should be no appreciable change in chemical environments of elements presented at the In_2S_3−Cu_2ZnSnS_4 interface before and after the preheating treatment.

Since the rate of Ar^+ etching in the present condition was approximately 4 nm min^{-1} (see Experimental Section), more than 100 nm thickness of the upper parts of these films, i.e.,

DOI: 10.1021/acs.chemmater.5b04984
Chem. Mater. XXXX, XXX, XXX−XXX

most of the In_2S_3 layer, should be removed after Ar^+ etching for more than 25 min. However, intense In 3d peaks were still observed when the etching durations were more than 30 min, even without application of the post-heat treatment, as shown in Figure 2a. These results suggest that appreciable amounts of In_2S_3 components penetrated into the grain boundary of the polycrystalline Cu_2ZnSnS_4 film during the CBD process.

As has been predicted in the literature,[35] one of the probable events induced by the post-heating was diffusion of elements between In_2S_3 and Cu_2ZnSnS_4 in the vertical direction of the In_2S_3−Cu_2ZnSnS_4 stack. In order to examine the occurrence of such events, peak area ratios of Cu $2p_{3/2}$ to In $3d_{5/2}$ of $In_2S_3(90)/Cu_2ZnSnS_4$_w/o and $In_2S_3(90)/Cu_2ZnSnS_4$ _PH samples were plotted as a function of etching duration (Figure 2, right). As a result, there was almost no difference between these samples: there was almost no Cu component at the surface region (<ca. 60 nm) observed even after the post-heating, and slopes of the plots over the etching duration of 20 min were comparable. For the further evaluation of distributions of elements included in the In_2S_3−Cu_2ZnSnS_4 stack, depth profiles of Cu, In, S, Sn, and Zn elements were analyzed by using an auger electron microscope (AES). Figure 3 shows AES results on $In_2S_3(90)/Cu_2ZnSnS_4$_w/o and

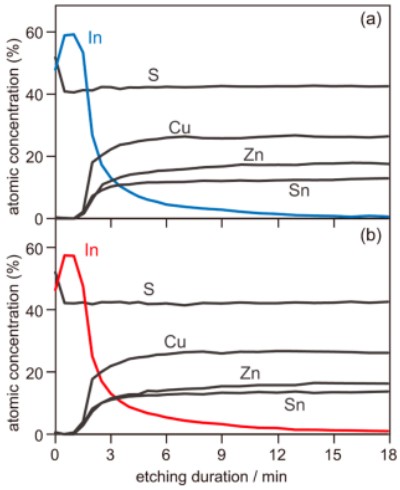

Figure 3. Depth profiles of elements in (a) $In_2S_3(90)/Cu_2ZnSnS_4$_w/o and (b) $In_2S_3(90)/Cu_2ZnSnS_4$ _PH films obtained by AES analyses.

$In_2S_3(90)/Cu_2ZnSnS_4$ _PH films. It is clear from the figure that there is almost no difference between the samples: all of the elements in both films had comparable distributions along with the vertical direction. Similar results were also obtained by depth profile analyses of In and Cu distributions in the solar cell in the region between the In_2S_3 buffer and the top part of the Cu_2ZnSnS_4 photoabsorber by using radio frequency glow discharge optical emission spectrometry (rf-GDOES): depth profiles of In and Cu components in $In_2S_3(90)/Cu_2ZnSnS_4$_PH were just changed slightly when compared to those in $In_2S_3(90)/Cu_2ZnSnS_4$_w/o (Figure S3). These results indicate that the present post-heat treatment did not significantly enhance interdiffusion of these elements.

Another noticeable feature of depth profiles obtained by AES analyses is that appreciable gradients of In distribution at the In_2S_3−Cu_2ZnSnS_4 interface was observed even for the sample without applying the post-heating. These results were in good agreement with the above XPS analyses (Figure 2), indicating penetration of In_2S_3 into the Cu_2ZnSnS_4 layer during the CBD process.

Since the atomic radius of In is similar to that of Sn, the formation energy of In_{Sn} (i.e., the Sn site in Cu_2ZnSnS_4 being replaced by In) is likely to be low. Hence, the post-heating was expected to result in formation of In_{Sn} defects due to atomic-scale diffusion of In into the Cu_2ZnSnS_4 layer (i.e., formation of In-doped Cu_2ZnSnS_4). Since amounts of valence electrons of In are lesser than those of Sn, In_{Sn} should lead to p-type doping in Cu_2ZnSnS_4.[47,48] In order to examine this, SCM was applied for cross sections of $In_2S_3(90)/Cu_2ZnSnS_4$_w/o and $In_2S_3(90)/Cu_2ZnSnS_4$ _PH films (Figure 4). In the

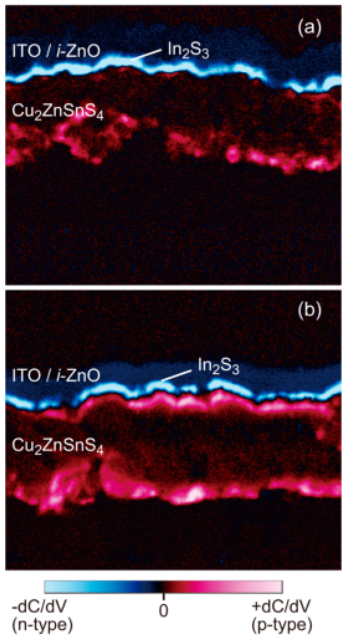

Figure 4. Cross-sectional SCM images of solar cells based on (a) In_2S_3/Cu_2ZnSnS_4_w/o and (b) In_2S_3/Cu_2ZnSnS_4_PH films.

$In_2S_3(90)/Cu_2ZnSnS_4$_w/o film, appreciably bright blue regions (i.e., largely negative dC/dV regions) were observed at the In_2S_3 part, as shown in Figure 4a, indicating that the CBD-deposited In_2S_3 layer had a relatively high donor concentration. For the Cu_2ZnSnS_4 layer near the In_2S_3−Cu_2ZnSnS_4 interface region in the film, relatively low acceptor concentration was confirmed by its dark appearance (i.e., giving a low dC/dV value). In contrast, the Cu_2ZnSnS_4 part near the In_2S_3−Cu_2ZnSnS_4 interface in the $In_2S_3(90)/Cu_2ZnSnS_4$_PH film was bright red, indicating that the part had a largely positive dC/dV value due to a high acceptor concentration (Figure 4b); the width of such an obvious p-type region was extended to ca. 300 nm from the In_2S_3−Cu_2ZnSnS_4 interface. Based on the results of CV measurement (Figure S4) of devices composed of $In_2S_3(90)/Cu_2ZnSnS_4$_w/o and $In_2S_3(90)/Cu_2ZnSnS_4$ _PH, acceptor densities of them were determined to be 1.2×10^{17} cm^{-3} and 2.2×10^{17} cm^{-3}, respectively: the

DOI: 10.1021/acs.chemmater.5b04984
Chem. Mater. XXXX, XXX, XXX−XXX

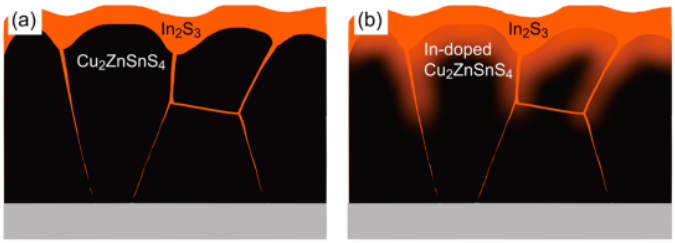

Figure 5. Schematic structural models of (a) $In_2S_3(90)/Cu_2ZnSnS_4$_w/o and (b) $In_2S_3(90)/Cu_2ZnSnS_4$ _PH films.

significant increase of the value induced by the post-heating is well consistent to the above SCM results.

The above results indicate that the application of post-heating of the In_2S_3–Cu_2ZnSnS_4 heterojunction induced interface enhancement of the p-type semiconductive property/acceptor concentration of the Cu_2ZnSnS_4 absorber due to the diffusion of In components existed as In_2S_3 at voids of Cu_2ZnSnS_4 grains, as schematically shown in Figure 5. The In doping would be beneficial for improving the built-in potential across the n-type buffer layer/Cu_2ZnSnS_4 junction, leading to improvement of V_{OC} of the solar cell. The results showing a significant improvement of V_{OC} in the final solar cell device (see Figure 1a) are attributed to change in the electric property of the Cu_2ZnSnS_4 film. This is the first time to strong evidence to prove such obvious enhancement of p-type doping intensity of Cu_2ZnS[34] via In doping has been given.

Typical dark current density–voltage (J–V) curves of solar cells based on $In_2S_3(90)/Cu_2ZnSnS_4$_w/o and $In_2S_3(90)/Cu_2ZnSnS_4$_PH films are shown in Figure 6. Ideality factor (n)

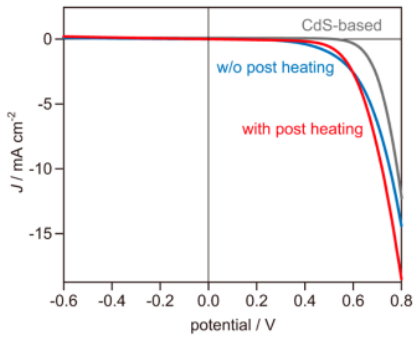

Figure 6. Dark J–V curves of solar cells based on (blue) In_2S_3/Cu_2ZnSnS_4_w/o, (red) In_2S_3/Cu_2ZnSnS_4_PH films, and (gray) the CdS/Cu_2ZnSnS_4-based solar cell. The detailed device properties of the CdS/Cu_2ZnSnS_4-based cell were given previously.[22]

and saturation current density (J_s) were estimated by fitting their dark J–V curves to the standard diode equation:

$$J = J_s\{\exp(qV/nkT) - 1\} \quad (1)$$

where q, k, and Tdenote elementary charge, Boltzmann constant, and temperature, respectively. As expected from the above-described results, the device based on the $In_2S_3(90)/Cu_2ZnSnS_4$_PH film had a relatively low n value (2.79) compared to that of the $In_2S_3(90)/Cu_2ZnSnS_4$_w/o-based device (3.1) owing to its better electrical rectification in the forward applied bias region. These results suggest effective reduction of the recombination current through the Shockley–Read–Hall recombination path achieved by reducing deep defects at the In_2S_3–Cu_2ZnSnS_4 heterointerface when applying the post-heat treatment. The lowering of the n value for the device based on the $In_2S_3(90)/Cu_2ZnSnS_4$_PH film also implies a successful decrease in series resistance (R_s) by applying the post-heat treatment, leading to improvements of J_{SC} and FF. As discussed above, the appreciable increase in acceptor density of the p-type Cu_2ZnSnS_4 layer would contribute to improvement of the conductivity of the Cu_2ZnSnS_4 layer. On the other hand, a higher J_s value was obtained for the device based on the $In_2S_3(90)/Cu_2ZnSnS_4$_PH film (7×10^{-7} mA cm^{-2}) than for the device based on the $In_2S_3(90)/Cu_2ZnSnS_4$_w/o film (1.4×10^{-6} mA cm^{-2}). These results indicate a significant dark current flow of the $In_2S_3(90)/Cu_2ZnSnS_4$_PH-based device in the reversed applied bias region due to the enhancement of the shunt induced by the post-heat treatment. It should also be noted that the thus-obtained n and J_s values of the present device was much larger than the device based on the CdS/Cu_2ZnSnS_4 film (i.e., n and J_s value of our best device composed of the CdS/Cu_2ZnSnS_4 film[22] determined from its dark J–V curve (given in Figure 4) to be 2.29 and 3×10^{-8} mA cm^{-2}, respectively. The relatively high n and J_s values of our In_2S_3/Cu_2ZnSnS_4 solar cell implies strong space charge region (SCR) recombination or that the tunneling enhanced interface recombination would be the dominant limiting factor. Hence, we can expect further improvement of device parameters of the present solar cell by improvement of the device quality and interfacial condition to suppress shunt and recombination.

Figure 7 shows external quantum efficiency (EQE) spectra of solar cells based on $In_2S_3(90)/Cu_2ZnSnS_4$_w/o and $In_2S_3(90)/Cu_2ZnSnS_4$_PH films. The spectra showed similar shapes, i.e., steep rises in the ultraviolet (UV)-blue region (<400 nm), maximum at ca. 450 nm, and gradual decreases to their onsets at around 850–960 nm. For the usual device based on the CdS/Cu_2ZnSnS_4 film, an appreciable drop of the EQE response was observed in the wavelength shorter than ca. 500 nm due to photoabroption of the CdS buffer layer.[15−24] As discussed in our previous reports,[37,38] transmittance spectra of In_2S_3 and CdS films deposited by the same CBD process on a glass substrate indicated that the In_2S_3 film had much higher transmittance than that of the CdS film because of its low photoabsorption coefficient derived from its indirect semiconductive property. Thus, the use of In_2S_3 instead of CdS should be advantageous for efficient utilization of sunlight of the blue region.

By comparison of the EQE spectra for solar cells based on $In_2S_3(90)/Cu_2ZnSnS_4$_PH and $In_2S_3(90)/Cu_2ZnSnS_4$_w/o films, moreover, good carrier collection efficiency of the former

DOI: 10.1021/acs.chemmater.5b04984
Chem. Mater. XXXX, XXX, XXX−XXX

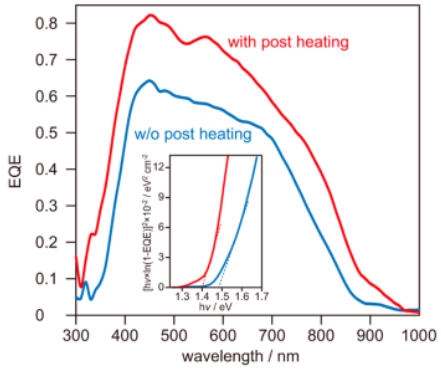

Figure 7. EQE spectra of solar cells based on (blue) In_2S_3/Cu_2ZnSnS_4_w/o and (red) In_2S_3/Cu_2ZnSnS_4_PH films. Inset shows plots of $h\nu\{\ln(1 - EQE)\}]^2$ versus $h\nu$ to determine E_g values of Cu_2ZnSnS_4 absorbers in these devices.

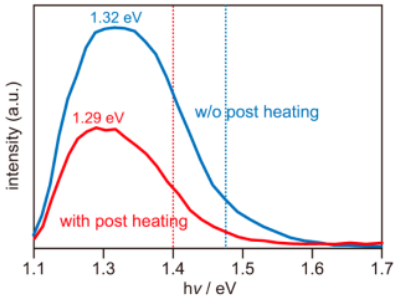

Figure 8. PL peak spectra of (bule) In_2S_3/Cu_2ZnSnS_4_w/o and (red) In_2S_3/Cu_2ZnSnS_4_PH films. Dotted lines indicate E_g values of Cu_2ZnSnS_4 in these films determined by above EQE analyses.

$In_2S_3(90)$/Cu_2ZnSnS_4_PH-based device in the entire wavelength region was confirmed when compared to the EQE spectrum of the device based on the latter $In_2S_3(90)$/Cu_2ZnSnS_4_w/o film, as expected from significant improvement of J_{SC} of the device. However, regarding the EQE drop observed in the intermediate wavelength region (ca. 450−700 nm), the best device showed a relatively steep drop compared to the $In_2S_3(90)$/Cu_2ZnSnS_4_w/o-based device. Since the Cu_2ZnSnS_4 film in the best device had relatively high carrier density (see above), the width of the depletion region of the Cu_2ZnSnS_4 film close to the In_2S_3−Cu_2ZnSnS_4 heterointerface should be shortened. Although the carrier doping should improve V_{OC}, the observed appreciable reduction of carrier collection efficiency was attributable to such an affect.

Another noticeable feature is that the EQE onset of the solar cell based on $In_2S_3(90)$/Cu_2ZnSnS_4_PH showed a significant shift to the longer wavelength region. The band gap energy (E_g) of the Cu_2ZnSnS_4 film estimated from the EQE data by applying extrapolation of the $[h\nu\{\ln(1 - EQE)\}]^2$−$h\nu$ plot to the $h\nu$ axis was 1.40 eV, while E_g of Cu_2ZnSnS_4 in $In_2S_3(90)$/Cu_2ZnSnS_4_w/o was 1.47 eV (inset of Figure 7). Since the observed photocurrent should be generated primarily in the depletion region of the Cu_2ZnSnS_4 film close to the In_2S_3−Cu_2ZnSnS_4 heterointerface, the observed reduction of E_g would have resulted from the diffusion of In into the Cu_2ZnSnS_4 layer. This hypothesis was supported by the fact that such a shift of the EQE onset was not observed for the cell based on the CdS/Cu_2ZnSnS_4 film even after applying the same post-heat treatment (data not shown).

Figure 8 shows photoluminescence (PL) spectra of $In_2S_3(90)$/Cu_2ZnSnS_4 and $In_2S_3(90)$/Cu_2ZnSnS_4_PH films measured at room temperature. The vertical lines in the figure indicate E_g values estimated from the above EQE spectra. The PL spectrum of $In_2S_3(90)$/Cu_2ZnSnS_4_w/o exhibited an asymmetry-shaped broad peak with peak energy of ca. 1.32 eV, similar to the spectrum obtained by a Cu_2ZnSnS_4 single crystal.[39,40] The observed smaller peak energy than the E_g value indicates the existence of band-tail states derived from high densities of donor and acceptor states such as Zn_{Cu} and Cu_{Zn}.[41] The peak energy of the $In_2S_3(90)$/Cu_2ZnSnS_4_PH film shifted toward the lower energy region, being consistent with the red shift of E_g estimated from the above EQE spectrum, though the degree of energy shift was relatively small. Since similar degrees of dependence of defect-derived PL peak energies on E_g values were also observed for a $Cu_2ZnSn(S,Se)_4$ film with different S/(S + Se) content[42] as well as a chalcopyrite $AgInS_2$-based nanoparticle system,[43] the observed peak shift is an item of collateral evidence of the E_g shift induced by diffusion of In. Another possible explanation of the observed E_g shift was predicted by a theoretical investigation reported by Wei and co-workers:[29] the E_g narrowing was possibly induced by formation of a defect cluster composed of Sn on Zn site and Cu on Zn site (i.e., the Sn_{Zn}−Cu_{Zn} cluster). Although there is no experimental evidence at present, formation of the Sn_{Zn}−Cu_{Zn} cluster would be enhanced by In doping since the doped In forces out the Sn from its regular site in the Cu_2ZnSnS_4 crystal. Hence, the use of In diffusion would be a unique strategy of E_g engineering for the pure sulfide Cu_2ZnSnS_4 to approach the optimal bandgap (1.34 eV) energy for sunlight (AM1.5G) utilization[44] without using the highly toxic selenium and/or Cd as substituents for sulfur and Zn, respectively.[45,46] In addition, a decrease in peak intensity was also observed for the $In_2S_3(90)$/Cu_2ZnSnS_4_PH film compared to $In_2S_3(90)$/Cu_2ZnSnS_4_w/o, suggesting increment of nonradiative recombination channels induced as an negative effect of the post-heating used.

3.3. Electronic Structure of the In_2S_3−Cu_2ZnSnS_4 Junction. In order to examine the electronic structure of the In_2S_3−Cu_2ZnSnS_4 heterointerface of the $In_2S_3(90)$/Cu_2ZnSnS_4_PH film, relative energy positions of the valence band maximums (VBMs) of In_2S_3 and Cu_2ZnSnS_4 layers in the film were determined by XP spectroscopy using the method reported by Kraut and co-workers.[49] In this method, core level XP signals closest to VBMs were employed. Hence, in the present In_2S_3/Cu_2ZnSnS_4 heterojunction, Zn 3d and In 3d core level energies were evaluated by direct XPS analysis of the In_2S_3−Cu_2ZnSnS_4 heterointerface. Figure 9a shows typical XP spectra of the $In_2S_3(90)$/Cu_2ZnSnS_4_PH film at a shallow binding energy (BE) level region (<25 eV). Before the measurement, the film was bombarded by Ar^+ within a short duration (5 min) to expose a clean In_2S_3 surfaces. The thus-obtained film showed an intense peak derived from the In 4d core level with BE (BE_{In}) of 17.75 eV in addition to a weak broad spectrum in the valence band region. Assuming that the onset BE (0.42 eV) of the valence band spectrum is VBM of In_2S_3 (VBM_{In2S3}), the energy difference between BE_{In} and VBM_{In2S3} ($\Delta E_{CL\text{-}VBM}$ for the In_2S_3 buffer layer) was estimated to be 17.33 eV. After the surface of the $In_2S_3(90)$/Cu_2ZnSnS_4 film had been bombarded by Ar^+ for 30 min to be etched to some extent, a Zn 3d core level peak appeared in addition to the In

DOI: 10.1021/acs.chemmater.5b04984
Chem. Mater. XXXX, XXX, XXX−XXX

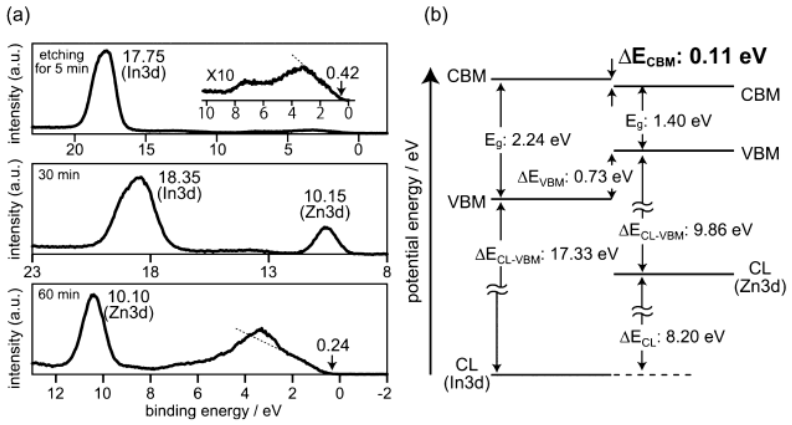

Figure 9. (a) XP spectra of $In_2S_3(90)/Cu_2ZnSnS_4$_PH in valence and shallow regions obtained after Ar^+ ion etching for 5, 30, and 60 min. (b) Energy diagram of the $In_2S_3(90)/Cu_2ZnSnS_4$_PH heterojunction estimated from XP spectroscopy and photoabsorption data.

4d peak due to the appearance of the In_2S_3/Cu_2ZnSnS_4 heterointerface. The difference in these two peaks, defined as ΔE_{CL}, was calculated to be 8.20 eV. When further Ar^+ ion etching for 60 min was performed, the XP spectrum would show the surface structure of the bottom Cu_2ZnSnS_4 layer doped with In components: the energy difference between BE of the Zn 3d core level and VBM of Cu_2ZnSnS ($\Delta E_{CL\text{-}VBM}$ for Cu_2ZnSnS_4) was determined to be 9.86 eV.

As shown in our previous study,[37,38] E_g values of the CBD-deposited In_2S_3 film were determined to be 2.24 eV. In accordance with the above discussion, moreover, E_g values of Cu_2ZnSnS_4 in $In_2S_3(90)/Cu_2ZnSnS_4$_PH (i.e., the In-doped Cu_2ZnSnS_4) of 1.40 eV was applied. Based on these values and the above parameters obtained by XP spectra, a schematic energy diagram of the $In_2S_3(90)/Cu_2ZnSnS_4$_PH interface was drawn down as shown in Figure 9b. The most significant result of the analyses of electronic structures is CBO (ΔE_{CBM}: defined as the potential energy of CBM of the buffer layer relative to that of Cu_2ZnSnS_4). In the present device, the thus-obtained ΔE_{CBM} value is slightly positive (0.11 eV). Being consistent with a few literature works,[32,33] the results indicate formation of a "notch-type" conduction band alignment for efficient suppression of the interface recombination, similar to the CdS-Cu(In,Ga)Se_2 interface of a highly efficient solar cell.[50,51] As has been reported in the literature,[32,33] the conduction band offset between CdS and Cu_2ZnSnS_4 ($\Delta CBM_{CdS\text{-}Cu2ZnSnS4}$) in the conventional CdS/Cu_2ZnSnS_4 junction has largely negative band offset, i.e., formation of a "cliff-type" conduction band alignment. Based on these facts, the present In_2S_3/Cu_2ZnSnS_4 heterojunction should be more favorable for increasing V_{OC} to suppress the V_{OC} deficit (defined as $E_g/q - V_{OC}$), while the achieved V_{OC} deficit (0.78 V) of the device was still slightly larger than that of the previously reported device based on the $CdS-Cu_2ZnSnS_4$ junction (0.73 V).

4. CONCLUSION

In summary, a solar cell based on electrodeposited Cu_2ZnSnS_4 and a Cd-free In_2S_3 buffer layer with maximum conversion efficiency of 6.9% was obtained by applying a post-heat treatment to the thus-formed $In_2S_3-Cu_2ZnSnS_4$ heterojunction. Due to the relatively high transparency of In_2S_3 compared to that of CdS, the EQE response in the short wavelength region was improved. Moreover, enhancement of the replacement of the Sn component by In in the Cu_2ZnSnS_4 layer induced by the post-heating resulted in an obvious increase in acceptor concentration of the Cu_2ZnSnS_4 film close to the $In_2S_3-Cu_2ZnSnS_4$ heterointerface. The In doping into Cu_2ZnSnS_4 also induced a change in the EQE response: E_g of Cu_2ZnSnS_4 was reduced by the In doping. As a result, appreciably large J_{SC} was obtained. Moreover, the $In_2S_3-Cu_2ZnSnS_4$ junction was found to be a more preferable notch-type CBO, apart from the usual $CdS-Cu_2ZnSnS_4$ junction having a cliff-type CBO. Therefore, the solar cell based on the $In_2S_3-Cu_2ZnSnS_4$ junction is promising to overcome the currently saturated efficiencies of the standard pure sulfide Cu_2ZnSnS_4-based solar cell by various suitable optimizations.

■ ASSOCIATED CONTENT

Supporting Information

The Supporting Information is available free of charge on the ACS Publications website at DOI: 10.1021/acs.chemmater.5b04984.

A cross-sectional SEM image of the 90 nm-thick In_2S_3-deposited CZTS solar cell, XP spectra of Sn 3d, Zn 2p, and O 1s core levels in In_2S_3/Cu_2ZnSnS_4_w/o and In_2S_3/Cu_2ZnSnS_4_PH films after Ar^+ etching for various durations, CV plots of solar cells based on In_2S_3/Cu_2ZnSnS_4_w/o and In_2S_3/Cu_2ZnSnS_4_PH films, and rf-GDOES profiles of In and Cu components in In_2S_3/Cu_2ZnSnS_4_w/o and In_2S_3/Cu_2ZnSnS_4_PH films (PDF)

■ AUTHOR INFORMATION

Corresponding Author

*(S.I.) E-mail: s-ikeda@center.konan-u.ac.jp.

Present Address

(S.I.) Department of Chemistry, Konan University 8-9-1 Okamoto, Higashinada, Kobe 658-8501, Japan.

Notes

The authors declare no competing financial interest.

DOI: 10.1021/acs.chemmater.5b04984
Chem. Mater. XXXX, XXX, XXX−XXX

■ ACKNOWLEDGMENTS

This work was carried out as part of a program supported by NEDO Japan. This work was also supported by a Grant-in-Aid for Scientific Research on Innovative Areas (All Nippon Artificial Photosynthesis Project for Living Earth) and a Grant-in-Aid for Scientific Research (B) from MEXT Japan. Feng Jiang is acknowledged for JSPS Postdoctoral Fellowship.

■ REFERENCES

(1) Katagiri, H.; Saitoh, K.; Washio, T.; Shinohara, H.; Kurumadani, T.; Miyajima, S. Development of thin film solar cell based on Cu_2ZnSnS_4 thin films. *Sol. Energy Mater. Sol. Cells* **2001**, *65*, 141−148.

(2) Katagiri, H.; Jimbo, K.; Maw, W. S.; Oishi, K.; Yamazaki, M.; Araki, H.; Takeuchi, A. Development of CZTS-based thin film solar cells. *Thin Solid Films* **2009**, *517*, 2455−2460.

(3) Riha, S. C.; Parkinson, B. A.; Prieto, A. L. Solution-based synthesis and characterization of Cu_2ZnSnS_4 nanocrystals. *J. Am. Chem. Soc.* **2009**, *131*, 12054−12055.

(4) Watjen, J. T.; Scragg, J. J.; Ericson, T.; Edoff, M.; Platzer-Bjorkman, C. Secondary compound formation revealed by transmission electron microscopy at the Cu_2ZnSnS_4/Mo interface. *Thin Solid Films* **2013**, *535*, 31−34.

(5) Siebentritt, S.; Schorr, S. Kesterites- a challenging materials for solar cells. *Prog. Photovoltaics* **2012**, *20*, 512−519.

(6) Kato, T.; Hiroi, H.; Sakai, N.; Muraoka, S.; Sugimoto, H. Characterization of front and back interfaces on Cu_2ZnSnS_4 thin film solar cells. *Proc. of 27th European Photovoltaic Solar Energy Conference and Exhibition* **2012**, 2236−2239.

(7) Sugimoto, H.; Liao, C.; Hiroi, H.; Sakai, N.; Kato, T. Life time improvement for high efficiency Cu_2ZnSnS_4 submodules. *Proc. of 39th IEEE Photovoltaic Specialists Conference* **2013**, 3208−3211.

(8) Tajima, S.; Itoh, T.; Hazama, H.; Ohishi, K.; Asahi, R. Improvement of the open-circuit voltage of Cu_2ZnSnS_4 cells using a two-layered process. *Proc. of 40th IEEE Photovoltaic Specialists Conference* **2014**, 431−434.

(9) Scragg, J.; Kubart, T.; Watjen, J.; Ericson, T.; Linnarsson, M.; Platzer-Bjorkman, C. Effects of back contact instability on Cu_2ZnSnS_4 devices and Processes. *Chem. Mater.* **2013**, *25*, 3162−3171.

(10) Collord, A.; Hillhouse, H. Composition control and formation pathway of CZTS and CZTGS nanocrystal inks for kesterite solar cells. *Chem. Mater.* **2015**, *27*, 1855−1862.

(11) Jiang, C.; Liu, W.; Talapin, D. Role of precursor reactivity in crystallization of solution-processed semiconductors: the case of Cu_2ZnSnS_4. *Chem. Mater.* **2014**, *26*, 4038−4043.

(12) Cho, J. W.; Ismail, A.; Park, S. J.; Kim, W.; Yoon, S.; Min, B. K. Synthesis of Cu_2ZnSnS_4 thin film by a precursor solution paste for thin film solar cell applications. *ACS Appl. Mater. Interfaces* **2013**, *5*, 4162−4165.

(13) Xin, H.; Katahara, J. K.; Braly, I. L.; Hillhouse, H. W. 8% Efficient $Cu_2ZnSn(S,Se)_4$ solar cells from redox equilibrated simple precursors in DMSO. *Adv. Energy Mater.* **2014**, *4*, 1301823.

(14) Scragg, J. J.; Dale, P. J.; Peter, L. M.; Zoppi, G.; Forbes, I. New routes to sustainable photovoltaics: evaluation of Cu_2ZnSnS_4 as an alternative absorber material. *Phys. Status Solidi B* **2008**, *245*, 1772−1778.

(15) Ennaoui, A.; Lux-Steiner, M.; Weber, A.; Abou-Ras, D.; Kötschau, I.; Schock, H. W.; Schurr, R.; Hölzing, A.; Jost, S.; Hock, R.; Voß, T.; Schulze, J.; Kirbs, A. Cu_2ZnSnS_4 thin film solar cell from electrodeposited precursors: novel low post-cost perspective. *Thin Solid Films* **2009**, *517*, 2511−2514.

(16) Ahmed, S.; Reuter, K. B.; Gunawan, O.; Guo, L.; Romankiw, L. T.; Deligianni, H. A high efficiency electrodeposited Cu_2ZnSnS_4 solar cell. *Adv. Energy Mater.* **2012**, *2*, 253−259.

(17) Wang, Y.; Wei, M.; Fan, F.; Zhuang, T.; Wu, L.; Yu, S.; Zhu, C. Phase-selective synthesis of Cu_2ZnSnS_4 nanocrystals through cation exchange for photovoltaic devices. *Chem. Mater.* **2014**, *26*, 5492−5498.

(18) Johnson, M. C.; Wrasman, C.; Zhang, X.; Manno, M.; Leighton, C.; Aydil, E. S. Self regulation of Cu/Sn ratio in the synthesis of Cu_2ZnSnS_4 films. *Chem. Mater.* **2015**, *27*, 2507−2514.

(19) Neuschitzer, M.; Sanchez, Y.; Olar, T.; Thersleff, T.; Lopez-Marino, S.; Oliva, F.; Espindola-Rodriguez, M.; Xie, H.; Placidi, M.; Izquierdo-Roca, V.; Lauermann, I.; Leifer, K.; Perez-Rodriguez, A.; Saucedo, E. Complex surface chemistry of kesterite: Cu/Zn reordering after low temperature postdeposition annealing and its role in high performance devices. *Chem. Mater.* **2015**, *27*, 5279−5287.

(20) Yang, W.; Miskin, C.; Carter, N.; Agrawal, R.; Stach, E. Compositional inhomogeneity of multinary semiconductor nanoparticles: a case study of Cu_2ZnSnS_4. *Chem. Mater.* **2014**, *26*, 6955−6962.

(21) Lin, Y.; Ikeda, S.; Septina, W.; Harada, T.; Matsumura, M.; Kawasaki, T. Mechanistic aspects of preheating effects of electrodeposited metallic precursors on structural and photovoltaic properties of Cu_2ZnSnS_4 thin films. *Sol. Energy Mater. Sol. Cells* **2014**, *120*, 218−225.

(22) Jiang, F.; Ikeda, S.; Harada, T.; Matsumura, M. Pure Sulfide Cu_2ZnSnS_4 Thin Film Solar Cells Fabricated by Preheating an Electrodeposited Metallic Stack. *Adv. Energy Mater.* **2014**, *4*, 1301381.

(23) Jiang, F.; Ikeda, S.; Harada, T.; Ide, A.; Mochihara, K.; Yoshino, T.; Matsumura, M. Fabrication of an efficient electrodeposited Cu_2ZnSnS_4-based solar cells with more than 6% conversion efficiency using a sprayed Ga-doped ZnO window layer. *RSC Adv.* **2014**, *4*, 24351−24355.

(24) Jiang, F.; Ikeda, S.; Tang, Z.; Minemoto, T.; Septina, W.; Harada, T.; Matsumura, M. Impact of alloying duration of an electrodeposited Cu/Sn/Zn metallic stack on properties of Cu_2ZnSnS_4 absprbers for thin-film solar cells. *Prog. Photovoltaics* **2015**, *23*, 1884−1895.

(25) Kornhuber, K.; Kavalakkatt, J.; Lin, X.; Ennaoui, A.; Lux-Steiner, M. In situ monitoring of electrophoretic deposition of Cu_2ZnSnS_4 nanocrystals. *RSC Adv.* **2013**, *3*, 5845−5850.

(26) Toyama, T.; Konishi, T.; Seo, Y.; Tsuji, R.; Terai, K.; Nakashima, Y.; Okamoto, H.; Tsutsumi, Y. Grain growth in Cu_2ZnSnS_4 thin film using Sn vapor transport for photovoltaic applications. *Appl. Phys. Express* **2013**, *6*, 075503.

(27) Dhakal, T. P.; Peng, C. Y.; Tobias, R. R.; Dasharathy, R.; Westgate, C. R. Characterization of a CZTS thin film solar cell grown by sputtering method. *Sol. Energy* **2014**, *100*, 23−30.

(28) Tajima, S.; Asahi, R.; Isheim, D.; Seidman, D. N.; Itoh, T.; Hasegawa, M.; Ohishi, K. Atom-probe tomographic study of interface of Cu_2ZnSnS_4 photovoltaic cells. *Appl. Phys. Lett.* **2014**, *105*, 093901.

(29) Chen, S.; Walsh, A.; Yang, J.; Gong, X.; Sun, L.; Yang, P.; Chu, J.; Wei, S. Compositional dependence of structural and electronic properties of $Cu_2ZnSn(S,Se)_4$ alloys for thin film solar cells. *Phys. Rev. B: Condens. Matter Mater. Phys.* **2011**, *83*, 125201.

(30) Bär, M.; Schubert, B. A.; Marsen, B.; Wilks, R. G.; Pookpanratana, S.; Blum, M.; Krause, S.; Unold, T.; Yang, W.; Weinhardt, L.; Heske, C.; Schock, H. W. Impact of KCN etching on the chemical and electronic surface structure of Cu_2ZnSnS_4 thin-film solar cell absorbers. *Appl. Phys. Lett.* **2011**, *99*, 222105.

(31) Santoni, A.; Biccari, F.; Malerba, C.; Valentini, M.; Chierchia, R.; Mittiga, A. Valence band offset at the CdS/Cu_2ZnSnS_4 interface probed by x-ray photoelectron spectroscopy. *J. Phys. D: Appl. Phys.* **2013**, *46*, 175101.

(32) Yan, C.; Liu, F.; Song, N.; Ng, B. K.; Stride, J. A.; Tadich, A.; Hao, X. Band alignments of different buffer layers (CdS, Zn (O, S), and In_2S_3) on Cu_2ZnSnS_4. *Appl. Phys. Lett.* **2014**, *104*, 173901.

(33) Barkhouse, D. A. R.; Haight, R.; Sakai, N.; Hiroi, H.; Sugimoto, H.; Mitzi, D. B. Cd-free buffer layer materials on $Cu_2ZnSn(S_xSe_{1-x})_4$: Band alignments with ZnO, ZnS, and In_2S_3. *Appl. Phys. Lett.* **2012**, *100*, 193904.

(34) Sandoval-Paz, M. G.; Sotelo-Lerma, M.; Valenzuela-Jáuregui, J. J.; Flores-Acosta, M.; Ramirez-Bon, R. Structural and optical studies on thermal-annealed In_2S_3 films prepared by the chemical bath deposition technique. *Thin Solid Films* **2005**, *472*, 5−10.

DOI: 10.1021/acs.chemmater.5b04984
Chem. Mater. XXXX, XXX, XXX−XXX

(35) Hiroi, H.; Sakai, N.; Muraoka, S.; Katou, T.; Sugimoto, H. Development of high efficiency Cu_2ZnSnS_4 submodule with Cd-free buffer layer. *Proc. of 38th IEEE Photovoltaic Specialists Conference* **2012**, 1811−1814.
(36) Rajeshmon, V. G.; Poornima, N.; Sudha Kartha, C.; Vijayakumar, K. P. Modification of the optoelectronic properties of sprayed In_2S_3 thin films by indium diffusion for application as buffer layer in CZTS based solar cell. *J. Alloys Compd.* **2013**, *553*, 239−244.
(37) Gunawan; Septina, W.; Ikeda, S.; Harada, T.; Minegishi, T.; Domen, K.; Matsumura, M. Platinum and indium sulfide-modified $CuInS_2$ as efficient photocathodes for photoelectrochemical water splitting. *Chem. Commun.* **2014**, *50*, 8941−8943.
(38) Gunawan; Septina, W.; Harada, T.; Nose, Y.; Ikeda, S. Investigation of the Electric Structures of Heterointerfaces in Pt-and In_2S_3-Modified $CuInS_2$ Photocathodes Used for Sunlight-Induced Hydrogen Evolution. *ACS Appl. Mater. Interfaces* **2015**, *7*, 16086−16092.
(39) Phuong, L. Q.; Okano, M.; Yamada, Y.; Nagaoka, A.; Yoshino, K.; Kanemitsu, Y. Photocarrier localization and recombination dynamics in Cu_2ZnSnS_4 single crystals. *Appl. Phys. Lett.* **2013**, *103*, 191902.
(40) Phuong, L. Q.; Okano, M.; Yamada, Y.; Nagaoka, A.; Yoshino, K.; Kanemitsu, Y. Temperature-dependent photocarrier recombination dynamics in Cu_2ZnSnS_4. *Appl. Phys. Lett.* **2014**, *104*, 081907.
(41) Romero, M. J.; Du, H.; Teeter, G.; Yan, Y.; Al-Jassim, M. M. Comparative study of the luminescence and intrinsic point defects in the kesterite Cu_2ZnSnS_4 and chalcopyrite $Cu(In,Ga)Se_2$ thin films used in photovoltaic applications. *Phys. Rev. B: Condens. Matter Mater. Phys.* **2011**, *84*, 165324.
(42) Hironiwa, D.; Sakai, N.; Kato, T.; Sugimoto, H.; Tang, Z.; Chantana, J.; Minemoto, T. Impact of annealing treatment before buffer layer deposition on $Cu_2ZnSn(S,Se)_4$ solar cells. *Thin Solid Films* **2015**, [illegible], 151−153.
(43) Torimoto, T.; Kameyama, T.; Kuwabata, S. Photo-functional Materials Fabricated with Chalcopyrite-type Smiconductor Nanoparticles Composed of $AgInS_2$ and Its Solid Solution. *J. Phys. Chem. Lett.* **2014**, *5*, 336−347.
(44) Shockley, W.; Queisser, H. J. Detailed Balance Limit of Efficiency of pn Junction Solar Cells. *J. Appl. Phys.* **1961**, *32*, 510−519.
(45) Maeda, T.; Nakamura, S.; Wada, T. First-Principles Study on Cd Doping in Cu_2ZnSnS_4 and $Cu_2ZnSnSe_4$. *Jpn. J. Appl. Phys.* **2012**, *51*, 10NC11.
(46) Zhao, W.; Wang, G.; Tian, Q.; Huang, Gao, S.; Pan, D. Solution-processed $Cu_2CdSn(S, Se)_4$ thin film solar cells. *Sol. Energy Mater. Sol. Cells* **2015**, *133*, 15-
(47) Kuo, D.; Tsega, M. Electrical conduction and mobility enhancement in p-type In-doped $Cu_2ZnSnSe_4$ bulks. *Jpn. J. Appl. Phys.* **2014**, *53*, 035801.
(48) Kim, J.; Hiroi, H.; Todorov, T. K.; Gunawan, O.; Kuwahara, M.; Gokmen, T.; Nair, D.; Hopstaken, M.; Shin, B.; Lee, Y. Wang, W.; Sugimoto, H.; Mitzi, D. B. High Efficiency $Cu_2ZnSn(S,Se)_4$ Solar Cells by Applying a Double In_2S_3/CdS Emitter. *Adv. Mater.* **2014**, *26*, 7427−7431.
(49) Kraut, E. A.; Grant, R. W.; Waldrop, J. R.; Kowalczyk, S. P. Precise Determination of the Valence-Band Edge in X-Ray Photoemission Spectra: Application to Measurement of Semiconductor Interface Potentials. *Phys. Rev. Lett.* **1980**, *44*, 1620−1623.
(50) Minemoto, T.; Matsui, T.; Takakura, H.; Hamakawa, Y.; Negami, T.; Hashimoto, Y.; Uenoyama, T.; Kitagawa, M. Precise Determination of the Valence-Band Edge in X-Ray Photoemission Spectra: Application to Measurement of Semiconductor Interface Potentials. *Sol. Energy Mater. Sol. Cells* **2001**, *67*, 83−88.
(51) Minemoto, T.; Hashimoto, Y.; Shams-Kolahi, W.; Satoh, T.; Negami, T.; Takakura, H.; Hamakawa, Y. Control of conduction band offset in wide-gap $Cu(In,Ga)Se_2$ solar cells. *Sol. Energy Mater. Sol. Cells* **2003**, *75*, 121−126.

DOI: 10.1021/acs.chemmater.5b04984
Chem. Mater. XXXX, XXX, XXX−XXX

'Effect of Indium Doping on Surface Optoelectrical Properties of Cu2ZnSnS4 Photoabsorber and Interfacial/Photovoltaic Performance of Cadmium Free In2S3/Cu2ZnSnS4 Heterojunction Thin Film Solar Cell

ORIGINALITY REPORT

10%	5%	7%	2%
SIMILARITY INDEX	INTERNET SOURCES	PUBLICATIONS	STUDENT PAPERS

PRIMARY SOURCES

1	Miara, Lincoln James, Shyue Ping Ong, Yifei Mo, William Davidson Richards, Youngsin Park, Jae-Myung Lee, Hyo Sug Lee, and Gerbrand Ceder. "Effect of Rb and Ta doping on the ionic conductivity and stability of the garnet Li7+2x-y(La3-xRbx)(Zr2-yTay)O12 (0≤x≤0.375, 0≤y≤1) superionic conductor – a first principles investigation", Chemistry of Materials, 2013. Publication	1%
2	Kameyama, Tatsuya, Yusuke Douke, Hiroko Shibakawa, Masahide Kawaraya, Hiroshi Segawa, Susumu Kuwabata, and Tsukasa Torimoto. "Widely-Controllable Electronic Energy Structure of ZnSe-AgInSe2 Solid Solution Nanocrystals for Quantum Dot-Sensitized Solar Cells", The Journal of Physical Chemistry C Publication	<1%

3	Kamiya, Yukiko, and Hiroyuki Asanuma. "Light-Driven DNA Nanomachine with a Photoresponsive Molecular Engine", Accounts of Chemical Research, 2014. Publication	<1 %
4	www.cambridge.org Internet Source	<1 %
5	www.science.gov Internet Source	<1 %
6	Francisco J. Espinosa-Faller, Dylan R. Conradson, Shannon C. Riha, Mary B. Martucci et al. " Neutron Diffraction and X-ray Absorption Fine Structure Evidence for Local Lattice Distortions and Aperiodic Antisite Substitution in Cu ZnSnS Nanoparticles ", The Journal of Physical Chemistry C, 2014 Publication	<1 %
7	dspace101.ansto.gov.au Internet Source	<1 %
8	koreauniv.pure.elsevier.com Internet Source	<1 %
9	aip.scitation.org Internet Source	<1 %
10	Maksym V. Kovalenko, Liberato Manna, Andreu Cabot, Zeger Hens et al. "Prospects of	<1 %

	Nanoscience with Nanocrystals", ACS Nano, 2015 Publication	
11	kwansei.repo.nii.ac.jp Internet Source	<1 %
12	Submitted to Yeungnam University Student Paper	<1 %
13	R. Aruna-Devi, M. Latha, S. Velumani, J. Santoyo-Salazar, J. Santos-Cruz. "Telescoping synthesis and goldilocks of CZTS nanocrystals", Materials Research Bulletin, 2019 Publication	<1 %
14	file.scirp.org Internet Source	<1 %
15	lib.dr.iastate.edu Internet Source	<1 %
16	Xulin He, Jiang Liu, Qinyan Ye, Kun Luo, Yidong Jiang, Cheng Liao, Liangqi Ouyang, Daming Zhuang, Jun Mei, Woonming Lau. "The role of Na incorporation in the low-temperature processed CIGS thin film solar cells using post deposition treatment", Journal of Alloys and Compounds, 2016 Publication	<1 %
17	www.fujipress.jp Internet Source	<1 %

18	Umezu, I.. "Optical properties of CdS nanocrystal covered by polymer chains on the surface", Microelectronic Engineering, 200304 Publication	<1 %
19	Charlotte Platzer-Björkman, Nicolas Barreau, Marcus Bär, Leo Choubrac et al. "Back and front contacts in kesterite solar cells: state-of-the-art and open questions", Journal of Physics: Energy, 2019 Publication	<1 %
20	Submitted to University of Venda Student Paper	<1 %
21	Bai, Sai, Yizheng Jin, Xiaoyong Liang, Zhizhen Ye, Zhongwei Wu, Baoquan Sun, Zaifei Ma, Zheng Tang, Jianpu Wang, Uli Würfel, Feng Gao, and Fengling Zhang. "Ethanedithiol Treatment of Solution-Processed ZnO Thin Films: Controlling the Intragap States of Electron Transporting Interlayers for Efficient and Stable Inverted Organic Photovoltaics", Advanced Energy Materials, 2014. Publication	<1 %
22	Yan-Fang Du, Jun-Qi Fan, Wen-Hui Zhou, Zheng-Ji Zhou, Jie Jiao, Si-Xin Wu. " One-Step Synthesis of Stoichiometric Cu ZnSnSe as Counter Electrode for Dye-Sensitized Solar Cells ", ACS Applied Materials & Interfaces, 2012	<1 %

	Publication	
23	china.iopscience.iop.org Internet Source	<1 %
24	worldwidescience.org Internet Source	<1 %
25	iopscience.iop.org Internet Source	<1 %
26	m.scirp.org Internet Source	<1 %
27	www.cheric.org Internet Source	<1 %
28	www.kiche.or.kr Internet Source	<1 %
29	www.seris.sg Internet Source	<1 %
30	www.springerprofessional.de Internet Source	<1 %
31	A. Hultqvist, M. Edoff, T. Törndahl. "Evaluation of Zn□Sn□O buffer layers for CuIn0.5Ga0.5Se2 solar cells", Progress in Photovoltaics: Research and Applications, 2011 Publication	<1 %
32	Graetzel, Michael, René A. J. Janssen, David B. Mitzi, and Edward H. Sargent. "Materials	<1 %

interface engineering for solution-processed photovoltaics", Nature, 2012.
Publication

33	Yu-Wen Cheng, Fu-Ling Tang, Hong-Tao Xue, Hong-Xia Liu, Bo Gao, Yu-Dong Feng. " Bonding and electronic properties of the Cu ZnSnS /WZ–ZnO interface from first-principles calculations ", Journal of Physics D: Applied Physics, 2016 Publication	<1 %
34	epjpv.epj.org Internet Source	<1 %
35	pubs.rsc.org Internet Source	<1 %
36	Hiroi, Homare, Yasuaki Iwata, Kyouhei Horiguchi, and Hiroki Sugimoto. "960-mV Open-Circuit Voltage Chalcopyrite Solar Cell", IEEE Journal of Photovoltaics, 2015. Publication	<1 %
37	Satoshi Iwatsuki, Yuki Kanamitsu, Hidetaka Ohara, Eisuke Watanabe, Koji Ishihara. "Higher reactivity of 3-pyridinium boronic acid compared with 3-pyridinium boronate ion toward 4-isopropyltropolone in acidic aqueous solution: fundamental reaction analyses for an effective organoboron-based chemosensor", Journal of Physical Organic Chemistry, 2012	<1 %

	Publication	
38	Udai P. Singh, Surya P. Patra. " Progress in Polycrystalline Thin-Film Cu(In,Ga) Solar Cells ", International Journal of Photoenergy, 2010 Publication	<1 %
39	Submitted to University College London Student Paper	<1 %
40	Zhuang, Houlong L., and Richard G Hennig. "Single-Layer Group-III Monochalcogenide Photocatalysts for Water Splitting", Chemistry of Materials, 2013. Publication	<1 %
41	idus.us.es Internet Source	<1 %
42	livrepository.liverpool.ac.uk Internet Source	<1 %
43	www.tandfonline.com Internet Source	<1 %
44	Lin, Ling-Yan, Jin-Ling Yu, Shu-Ying Cheng, and Pei-Min Lu. "Influence of Ag and Sn incorporation in In2S3 thin films", Chinese Physics B, 2015. Publication	<1 %
45	Marianna Kemell, Mikko Ritala, Markku Leskelä. " Thin Film Deposition Methods for	<1 %

CuInSe Solar Cells ", Critical Reviews in Solid State and Materials Sciences, 2005

Publication

Exclude quotes	Off	Exclude matches	Off
Exclude bibliography	Off		

'Effect of Indium Doping on Surface Optoelectrical Properties of Cu2ZnSnS4 Photoabsorber and Interfacial/Photovoltaic Performance of Cadmium Free In2S3/Cu2ZnSnS4 Heterojunction Thin Film Solar Cell

GRADEMARK REPORT

FINAL GRADE

/0

GENERAL COMMENTS

Instructor

PAGE 1

PAGE 2

PAGE 3

PAGE 4

PAGE 5

PAGE 6

PAGE 7

PAGE 8

PAGE 9

Comment 1

no comment